

Delayed γ Rays from Thermal-Neutron Fission of U^{235} and Pu^{239} †

A. C. BERICK, A. E. EVANS, AND J. A. MEISSNER

University of California, Los Alamos Scientific Laboratory, Los Alamos, New Mexico 87544

(Received 23 April 1969)

Measurements of the time dependence of delayed γ -ray activities from thermal-neutron fission of U^{235} and Pu^{239} have been performed with a plastic scintillation detector for the time interval 0.01–4.0 sec after fission. Absolute intensities were obtained by normalizing these data to the results of Fisher and Engle which cover the time interval 0.2–45.0 sec after fission. The present results are in satisfactory agreement with Griffin's theoretical extrapolations to the msec region.

I. INTRODUCTION

ABSOLUTE-energy spectra of delayed γ rays from thermal-neutron fission of U^{235} have been measured by Maienschein *et al.*,¹ for the time ranges 0.12–1.0 μ sec and 1.2–1550 sec after fission. Fisher and Engle² performed similar measurements for the fast-neutron fission of several fission isotopes in the time range 0.2–45.0 sec after fission. Relative intensities and some data on the energy spectra of delayed γ rays from the neutron fission of U^{235} and Pu^{239} were obtained by Walton and Sund^{3,4} for the time region 2 μ sec–30 msec. These last data were normalized to the theoretical extrapolation of Giffin,⁵ which were based on the data of Fisher and Engle² and the β -decay data of Armbruster and Meister⁶ for the thermal-neutron fission of U^{235} . More recent β -decay measurements⁷ have cast some doubt on the previous results and, thereby, on the absolute delayed- γ -ray intensities extrapolated by Griffin.

The purpose of the present work was to bridge the gap between the early-time measurements of Walton and Sund and the later-time data of Fisher and Engle. The time dependence of delayed- γ -ray activities from the thermal-neutron fission of U^{235} and Pu^{239} was measured with a plastic scintillation detector for times 0.01–4.0 sec after fission. These new intermediate-time data provide an independent basis (other than Griffin's work) for normalizing the relative delayed- γ -ray data which extend back to 2 μ sec to the absolute intensities given by Fisher and Engle. In addition, the new-yield data can shed some light on the discrepancy in the β -decay measurements (Refs. 6 and 7).

† Work performed under the auspices of the U. S. Atomic Energy Commission.

¹ F. C. Maienschein, R. W. Peele, W. Zobel, and T. A. Love, in *Proceedings of the Second International Conference on the Peaceful Uses of Atomic Energy* (United Nations, Geneva, 1958), Vol. 15, p. 366.

² P. C. Fisher and L. B. Engle, *Phys. Rev.* **134**, B796 (1964).

³ R. B. Walton and R. E. Sund, *Phys. Rev.* **178**, 1894 (1969).

⁴ R. E. Sund and R. B. Walton, *Phys. Rev.* **146**, 824 (1966).

⁵ J. J. Griffin, *Phys. Rev.* **134**, B817 (1964).

⁶ P. Armbruster and H. Meister, *Z. Physik* **170**, 274 (1962).

⁷ H. J. Specht and H. Seyfarth, *Proceedings of the Symposium on the Physics and Chemistry of Fission, Salzburg*, (International Atomic Energy Agency, Vienna, 1965), Vol. II.

II. EXPERIMENTAL ARRANGEMENT

The neutron source for this experiment was a dense-plasma focus device (DPF) shown schematically in Fig. 1. Since such a neutron source has not been commonly used in nuclear-physics research, the DPF will be described briefly here. This device has been developed and studied intensively by Mather and co-workers,^{8–12} and more recently by others.^{13–29}

When a high-current pulse of electrical energy is discharged into a coaxial tube as shown in Fig. 1, a current sheath forms between the bases of the electrodes.

⁸ J. W. Mather, in *Proceedings of a Conference on Plasma Physics and Controlled Nuclear Fusion Research, Culham, England, 1965* (International Atomic Energy Agency, Vienna, 1966), Vol. II.

⁹ J. W. Mather, in *Proceedings of a Seminar on Intense Neutron Sources, Santa Fe, 1966*, Vol. IV C, p. 1 (unpublished).

¹⁰ J. W. Mather, P. J. Bottoms, and A. H. Williams, in *Proceedings of the APS Topical Conference on Pulsed High-Density Plasmas, Los Alamos, 1967*, Paper C1 (unpublished).

¹¹ J. W. Mather, K. D. Ware, A. H. Williams, P. J. Bottoms, and J. P. Carpenter, *Bull. Am. Phys. Soc.* **13**, 1542 (1968).

¹² P. J. Bottoms, J. P. Carpenter, J. W. Mather, K. D. Ware, and A. H. Williams, *Bull. Am. Phys. Soc.* **13**, 1543 (1968).

¹³ E. H. Beckner, *Rev. Sci. Instr.* **38**, 507 (1967).

¹⁴ C. Patou, A. Simonnet and J. P. Watteau, Ref. 10, Paper C2.

¹⁵ C. A. Caoudeville, A. Tolas, and J. P. Watteau, Ref. 10, Paper C3.

¹⁶ E. H. Beckner, Ref. 10, Paper C4.

¹⁷ J. W. Long, N. J. Peacock, P. D. Wilcock, and R. J. Speer, Ref. 10, C 5.

¹⁸ D. A. Megkan, H. L. VanDassen, and G. G. Comisar, Ref., 10, Paper C6.

¹⁹ M. Bernstein, *Bull. Am. Phys. Soc.* **13**, 878 (1968).

²⁰ J. R. A. J. N. Castro, E. H. Beckner, and D. R. Smith, *Bull. Am. Phys. Soc.* **13**, 877 (1968).

²¹ V. Josephson, H. L. VanPassen, and M. H. Dazey, *Bull. Am. Phys. Soc.* **13**, 904 (1968).

²² J. H. Lee, H. Conrads, M. D. Williams, L. P. Shmo, H. Hermandsdorfer, and K. Kim, *Bull. Am. Phys. Soc.* **13**, 1543 (1968).

²³ E. H. Beckner and D. R. Smith, *Bull. Am. Phys. Soc.* **13**, 1543 (1968).

²⁴ J. P. Baconnet, G. Cesari, A. Coudeville, and J. P. Watteau, *Bull. Am. Phys. Soc.* **13**, 1543 (1968).

²⁵ G. Decker, D. Mayhall, O. Friedrich, and A. A. Dougal, *Bull. Am. Phys. Soc.* **13**, 1543 (1968).

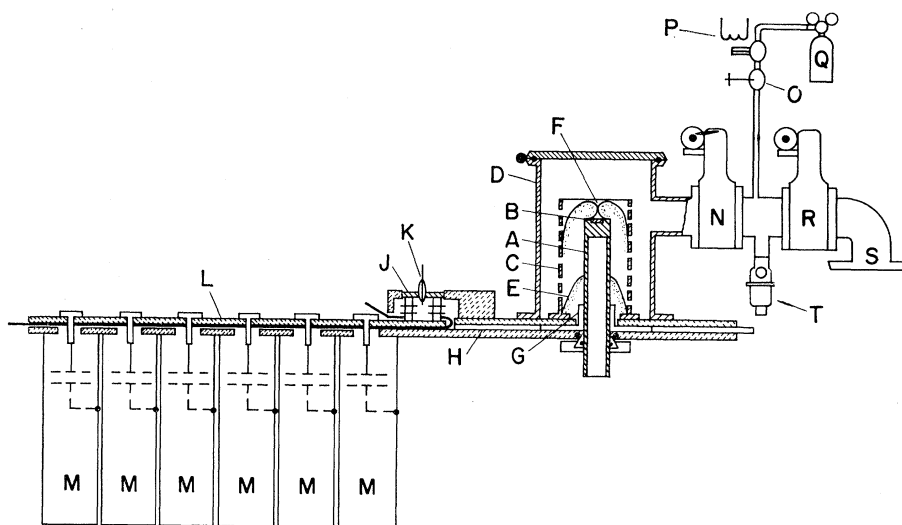
²⁶ E. L. Patterson, *Bull. Am. Phys. Soc.* **13**, 1543 (1968).

²⁷ G. G. Comisar, *Bull. Am. Phys. Soc.* **13**, 1544 (1968).

²⁸ D. L. Lafferty, D. C. Gates, and C. H. Hinrichs, *Bull. Am. Phys. Soc.* **13**, 1544 (1968).

²⁹ W. H. Bostick and L. Grunberger, *Bull. Am. Phys. Soc.* **13**, 1544 (1968).

FIG. 1. DPF neutron source:
 A: 7.5-cm diam \times 20-cm Cu inner electrode. B: W insert. C: Perforated Cu outer electrode. D: Stainless vacuum can. 35 \times 20-cm diam. E: Plasma sheath shortly after start of discharge. F: Plasma focus at moment of neutron production. G: 6.4-mm-thick Pyrex insulator. H: 6.4-mm-thick polyethylene spacer. J: Vacuum spark-gap assembly (there are 4 spark gaps, each one connecting three storage capacitors to the discharge gun). K: Initiating spark plug. L: Strip-line structure, consisting of 2.5-cm-thick Al plates and 0.5-mm Mylar insulation. M: 15 μ f, 20-kV low-inductance capacitors (twelve). N: Chamber valve. O: Needle valve. P: Solenoid valve. Q: Deuterium reservoir. R: Diffusion-pump valve. S: Diffusion-pump outlet. T: Roughing valve. The entire assembly is approximately 2.5 m long \times 75 cm wide \times 1 m high.



This current sheath is accelerated magnetohydrodynamically along the tube until it reaches the end of the inner electrode, whereupon the discharge collapses along the axis of the tube, heating and compressing the discharge gas to temperatures and pressures at which neutrons are produced by the $d-d$ reaction. The DPF used for the work reported in this paper was capable of producing bursts of $\sim 10^{10}$ $d-d$ neutrons during time intervals of 50–100 nsec. Such bursts were produced by discharging a bank of twelve 18-kV, 15- μ F, low-inductance capacitors through four vacuum-switch devices³⁰ into the discharge tube. The discharge tube was filled with deuterium at a pressure of 6–8 Torr. Repetition rates of approximately 1 per min were possible, the limiting factor being the time required to pump out and refill the vacuum switches after each shot and to recharge the storage capacitors. Under optimum conditions, the discharge-chamber gas, which took 3 min to change, would suffice for 40–50 shots.

A schematic drawing of the experimental setup used for the delayed γ -ray measurements is shown in Fig. 2. 2.5-MeV neutrons from the DPF were moderated by allowing them to pass into a 20 \times 17.5-cm polyethylene block in which the fission sample was embedded. The fission sample was centered 7.5 cm from the surface which was closest to the neutron source. The results of neutron-transport calculations indicated that the maximum thermal flux was located in this region and that 63% of the neutron flux near the sample position had energies less than 1 eV. The polyethylene block was

surrounded by a lead shield which had as its two basic functions the shielding of the beam monitor from the sample activity and the reflection of neutrons back into the moderator.

The fission samples were in the form of disks 5 cm in diameter and 0.25 mm thick. The Pu^{239} sample was enclosed in a 0.25-mm copper cladding. Sample compositions, as determined by spectrographic analysis, are given in Table I.

The delayed γ activity of the fission samples was measured with a 5 \times 5-cm cylinder of plastic scintillator which was mounted on an RCA 8575 photomultiplier tube and shielded by a steel cylinder 7.5 cm thick and 25 cm long. Since the primary goal of this measurement was the delayed γ -ray emission rate versus time (and not the energy spectrum), a plastic scintillator was selected instead of one of NaI to avoid the problem of neutron activation of the detector. The output of the photomultiplier tube was stretched and fed into a TMC 400-channel pulse-height analyzer operated in the multiscaler mode with 10-msec/channel. Sweeping of the multiscaler unit was initiated by a pulse generator which also provided the firing pulse for the DPF. The time delay between these two pulses was continuously variable from zero to 200 msec.

Total neutron output of the DPF was monitored by a Pb activation detector shown schematically in Fig. 2. This monitor consists of a 5 \times 5-cm plastic scintillator mounted on an RCA 8575 photomultiplier tube and surrounded by a 1-in.-thick Pb mantle.³¹ The 2.5-MeV

³⁰J. W. Mather and A. H. Williams, Rev. Sci. Instr. **31**, 279 (1960).

³¹L. Ruby and J. B. Recher, Nucl. Instr. Methods **53**, 290 (1967).

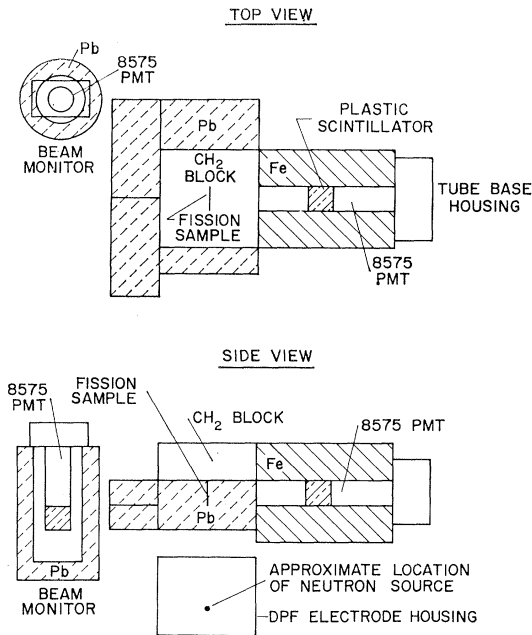


FIG. 2. Schematic diagram of the experimental setup used in the measurements of delayed γ -ray activities.

neutrons from the source activate the Pb via the $\text{Pb}^{207}(n, n')\text{Pb}^{207m}$ reaction, and the resultant 0.8-sec Pb^{207m} nuclei emit cascade γ rays with energies of 1.069 and 0.571 MeV, which are detected by the plastic scintillator. Because of the relatively short half-life of the Pb activity, the buildup of residual activity from previous irradiations was negligible as long as irradiation pulses were spaced at least 10 sec apart. The Pb activation detector was calibrated for absolute neutron yield using a silver-activation detector,³² which in turn was calibrated with $d(d, n)\text{He}^3$ neutrons from a Cockcroft-Walton generator, utilizing the associated-particle technique to determine absolute neutron fluxes. The response of the monitor was linear over the entire range of interest. Calibration points taken with and without the fission sample in place showed that there was no coupling between the monitor and the fission sample.

III. PROCEDURE

Delayed γ -ray activities were measured in three separate 2-h-runs for each sample. These runs were separated by measurements made without the sample in place to determine the background of short-lived activities in materials constituting the experimental environment. The long-lived background activities which accumulate from burst to burst were evaluated by measuring the counting rate immediately preceding each neutron burst and assuming this rate remained

constant during the 4.0-sec data-taking period. This assumption should be valid since the elapsed time between neutron bursts, 100 sec, was much greater than the data-taking interval. Over-all signal-to-background ratios were about 10 to 1 for the U^{235} runs and about 5 to 1 for the Pu^{239} runs.

Detection thresholds of both the neutron-beam monitor and the delayed- γ -ray detector were checked between runs using the Compton edge produced by a Cs^{137} source and a pulse-height analyzer operated in coincidence with the appropriate discriminator output. Thresholds were set at 380 keV for the delayed- γ -ray detector and 250 keV for the neutron-beam monitor.

In addition to the γ -activity time histories, pulse-height spectra were collected with the delayed γ detector for an early- and a late-time window for each sample. These pulse-height spectra were analyzed for time variations which could lead to changes in over-all γ detection efficiency, thereby distorting the activity-versus-time data. The early-time window extended from 0.05 to 0.10 sec after fission and the late-time window from 0.20 to 0.50 sec after fission. The late-time window is identical to the earliest time interval used by Fisher and Engle² in their absolute delayed- γ -ray-spectrum measurements. Since Fisher and Engle found that the delayed- γ -ray energy spectra were practically identical for the time domain ranging 0.20–45 sec after fission, the pulse-height measurements at only the two selected time intervals were considered sufficient for the present study.

IV. RESULTS

The pulse-height distributions obtained for U^{235} and Pu^{239} are shown in Figs. 3 and 4, respectively. The ordinates for the upper and lower curves were chosen for convenience, and are not related to the absolute γ activities for the respective periods. These pulse-height spectra were first examined to determine if efficiency corrections to the activity-versus-time data would be required. The spectra for U^{235} are sufficiently similar that a correction for the variation of detection efficiency with time was deemed unnecessary. In the case of Pu^{239} , the early-time spectrum is appreciably harder than the late-time spectrum, indicating the necessity for apply-

TABLE I. Composition of fission samples.

U^{235}		Pu^{239}	
Constituent	%	Constituent	%
U^{233}	<0.01	Pu^{237}	0.0022
U^{234}	1.09	Pu^{238}	0.0088
U^{235}	93.21	Pu^{239}	93.13
U^{236}	0.20	Pu^{240}	5.4
U^{238}	5.41	Pu^{241}	0.32
		Pu^{242}	0.017
		Ga	0.96
		Other	0.162

³² R. J. Lanter and D. E. Bannerman, Los Alamos Scientific Laboratory Report No. LA-3498-MS, 1966 (unpublished).

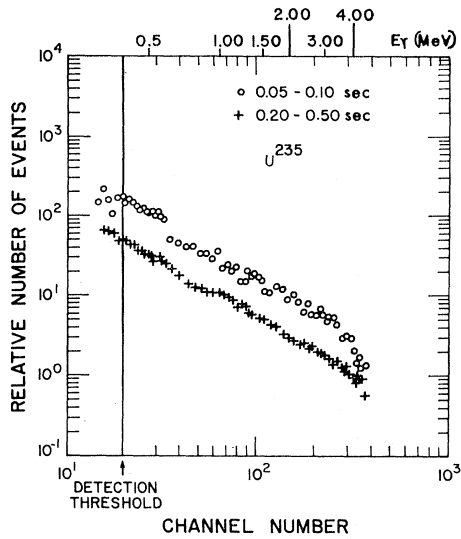


FIG. 3. γ -ray pulse-height spectra for early- and late-time intervals after U^{235} fission.

ing an efficiency correction of the Pu^{239} -activity data. This correction, which is described in detail in the Appendix, amounted to an average downward shift of 9% for the points in the plateau region (0.01–0.3 sec).

Figure 5 presents the results of the delayed- γ -activity measurements for U^{235} and Pu^{239} . The data for Pu^{239} have been corrected for the change in detection efficiency resulting from the observed spectral shift.

A least-squares exponential fit was obtained for each set of data, and the resulting fits were normalized to the photon-emission rates ($E_\gamma > 380$ keV) determined by Fisher and Engle.² The analytical representations of the present data, normalized to the absolute data of Fisher and Engle for $E_\gamma > 380$ keV, are presented in Fig. 6 and in Table II. The uncertainties in the present data,

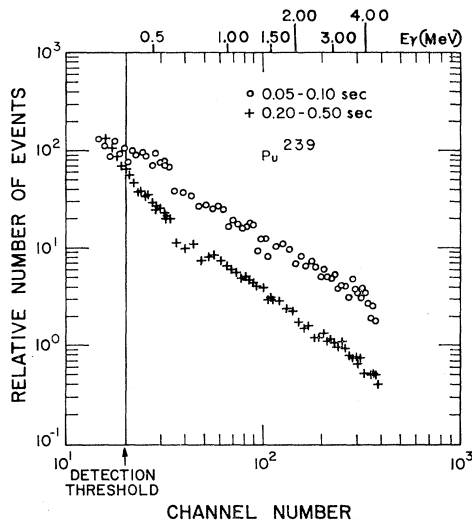


FIG. 4. γ -ray pulse-height spectra for early- and late-time intervals after Pu^{239} fission.

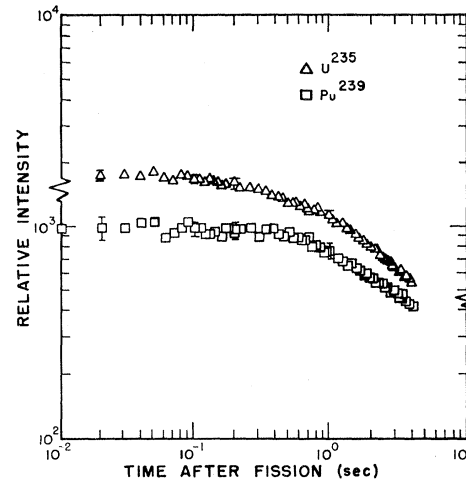


FIG. 5. Relative intensity of γ -ray activities versus time after the thermal-neutron fission of U^{235} and Pu^{239} . The data have been corrected for backgrounds and, in the case of Pu^{239} , for shifts in the energy spectrum. The discriminator integral bias setting was 380 keV.

which are indicated Fig. 6 by the bracketing curves, result primarily from the uncertainties in the data of Fisher and Engle which are propagated in the normalization. For comparison, the data of Fisher and Engle² and Griffin's extrapolations⁵ are also shown in Fig. 6. Griffin's results were converted from energy-emission rates (MeV/fission sec) to photon emission rates using the delayed- γ -ray spectra determined by Fisher and Engle. It is noteworthy that, although the Fisher-Engle data at 11.35 sec were not used for the normalization of the present data, the analytical fits derived from the

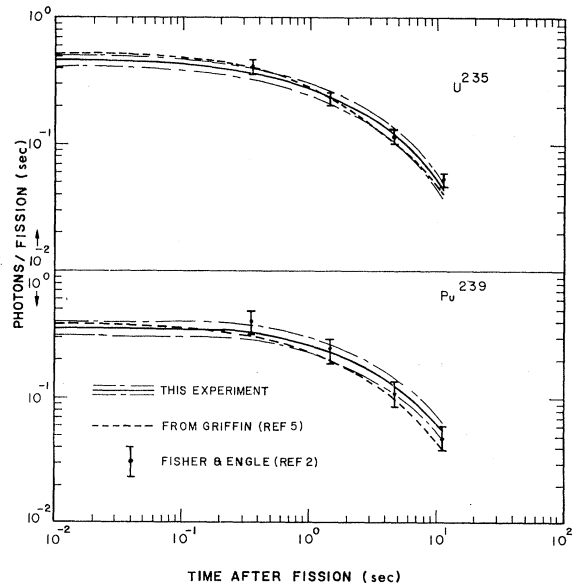


FIG. 6. Absolute intensity of γ -ray activity ($E_\gamma > 380$ keV) as a function of time after fission of U^{235} and Pu^{239} . The points are from Fisher and Engle (Ref. 2), and the dashed curves are the theoretical extrapolations by Griffin (Ref. 5).

TABLE II. Delayed γ activity.

Time after fission (sec)	γ 's/fission sec ($E_\gamma \geq 380$ keV)	
	U ²³⁵	Pu ²³⁹
0.01	0.448	0.350
0.05	0.438	0.348
0.10	0.430	0.346
0.20	0.402	0.343
0.30	0.381	0.340
0.40	0.362	0.332
0.50	0.345	0.317
0.60	0.329	0.302
0.70	0.314	0.289
0.80	0.301	0.278
0.90	0.289	0.267
1.00	0.278	0.257
1.20	0.259	0.241
1.40	0.242	0.228
1.60	0.228	0.216
1.80	0.216	0.206
2.00	0.205	0.197
2.50	0.181	0.179
3.00	0.164	0.165
3.50	0.149	0.154
4.00	0.137	0.143

present study appear to be valid even for such relatively late times.

In Fig. 7, the shapes of the β -emission curves given by Armbruster and Meister⁶ and by Specht and Seyfarth⁷ for the thermal-neutron fission of U²³⁵ are compared with the present delayed γ -ray data. The β -decay data, as well as the present delayed γ -ray results, were normalized to the delayed- γ -ray emission rates ($E_\gamma > 380$ keV) given by Fisher and Engle.² For this comparison it was assumed that the ratio of the emission rates of γ rays to β rays was constant over the relevant time range. The γ/β ratio obtained from the normalization to the Fisher-Engle data ($E_\gamma > 380$ keV) was 1.00 for the β -decay data of Ref. 6 and 1.32 for the data of Ref. 7. These ratios are constant to within 6% over the time range 0.35–11.35 sec after fission.

V. DISCUSSION

Examination of Fig. 6 shows that for both U²³⁵ and Pu²³⁹, the delayed- γ -ray activities obtained in this study are flatter (i.e., vary less with time) than the extrapolations by Griffin.⁵ Since the theoretical extrapolations are influenced by the shape of the β decay and since the β -decay curve obtained recently⁷ for thermal-neutron fission of U²³⁵ is flatter than that used by Griffin, it is expected that extrapolations based on the more recent β -decay data should be in better agreement with the present delayed γ -ray-decay curves. Nevertheless, Griffin's results for U²³⁵ are in good agreement with the present data, being only about 10% higher in the plateau region.

In the case of Pu²³⁹, Griffin's results, which were calculated using the parameters derived from the theoretical fits to the β - and γ -ray measurements for U²³⁵ fission, are appreciably lower than the data of Fisher and Engle for Pu²³⁹. If the decay curve calculated by Griffin were forced to fit the Fisher-Engle data for Pu²³⁹, then, as in the case of U²³⁵, the theoretical curve would be significantly higher in the plateau region than the present data.

The direct comparison of the shape of present U²³⁵-fission delayed- γ -ray decay with the corresponding β -emission data of Refs. 6 and 7 shown in Fig. 7, indicates that the more recent β -decay curve (Ref. 7) is in better agreement with the present results, providing, of course, that the assumption of a constant γ/β ratio over the relevant time range is valid.

In conclusion, this study indicates that Griffin's predictions of γ -ray activities in the time domain 0.0–0.10 sec after fission, although in satisfactory agreement with the present measurements, could possibly be improved by using recent U²³⁵ fission β -decay data to fix the parameters of the theory.

ACKNOWLEDGMENTS

The authors would like to acknowledge the help of Dr. R. B. Walton for suggesting this experiment and for many helpful suggestions during its performance. We wish also to thank Dr. G. R. Keepin for his continuing interest and cooperation in allowing the experiment to be performed. The many helpful suggestions of Dr. J. W. Mather and Dr. A. H. Williams with regard to the

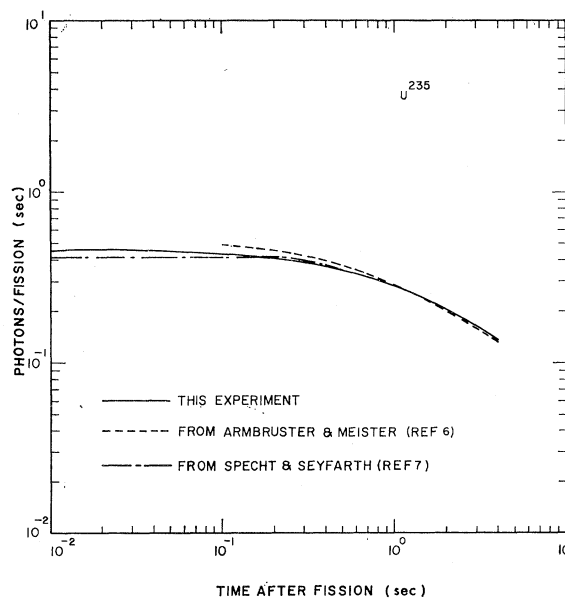


Fig. 7. Comparison of the shapes of the delayed γ -ray activity (from this investigation) and β activity (Ref. 6 and 7) following the thermal-neutron fission of U²³⁵. All the data shown were normalized to the U²³⁵-fission delayed- γ -ray data of Fisher and Engle² in the time interval 0.35–11.35 sec. It was assumed that the γ/β ratio was constant over the entire time range.

DPF during its building and developmental period is gratefully acknowledged. Finally, we would like to acknowledge the work and skill of G. M. Worth in helping to build the DPF.

APPENDIX: CALCULATION OF CHANGE IN DETECTION EFFICIENCY DUE TO ENERGY-SPECTRUM SHIFT FOR Pu^{239}

A. Photon-Detection Efficiency

The first step in the calculation was the computation of the photon-detection efficiency as a function of γ -ray energy. The calculation was performed as a function of the energy of the Compton edge, and it was assumed that the energy spectrum of Compton-scattered electrons was rectangular in shape. Under these circumstances the detection efficiency $\epsilon(E_i)$ can be written as

$$\epsilon(E_i) = [(E_i - E_b)/E_i] \{1 - \exp[-\mu_p(E_0)d]\} \\ \times \exp[-\mu_{CH_2}(E_0)t],$$

where E_i is the energy of the Compton edge, E_b is the detection threshold energy expressed as Compton energy, μ_p is the photon interaction coefficient in the scintillator, μ_{CH_2} is the photon interaction coefficient in the polyethylene block (see Fig. 1), E_0 is the initial photon energy, and d and t are the respective thicknesses of scintillator and polyethylene.

The first term is the detection efficiency for a photon which has interacted in the plastic scintillator; the second term is the probability for penetrating the polyethylene without interacting. Attenuation of γ rays through the fission samples was neglected since it affected less than 1% of the total γ -ray emission. The results are plotted in Fig. 8.

B. Unfolding of the Energy Spectra

It was assumed that the resultant pulse-height distributions are superpositions of individual Compton

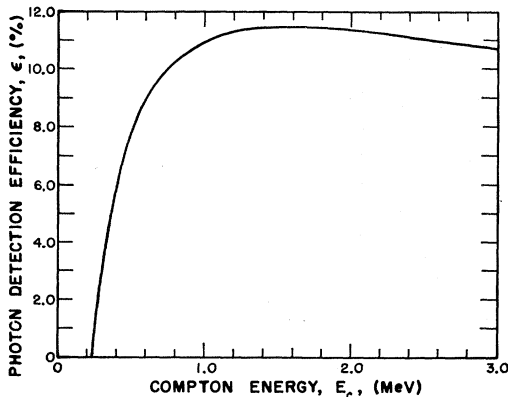


FIG. 8. Computed γ -ray detection efficiency (including attenuation by the moderator surrounding the fission sample). The independent variable is the maximum energy imparted to a Compton-scattered electron.

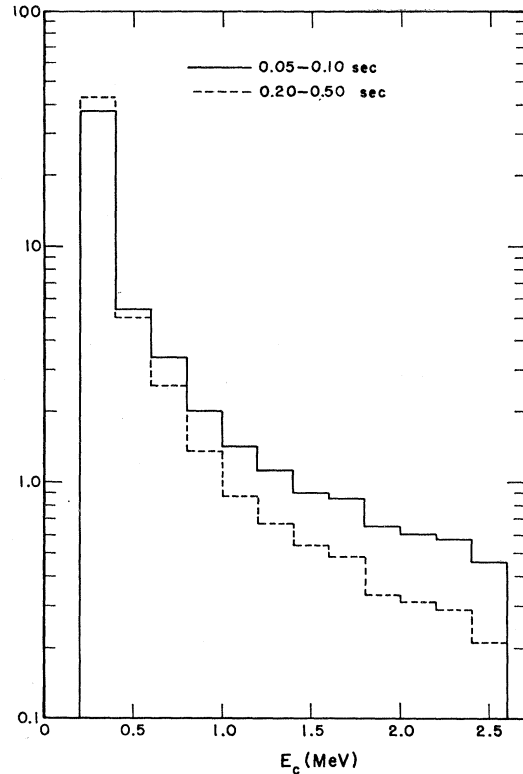


FIG. 9. Unfolded energy spectra for Pu^{239} . The independent variable is the maximum energy imparted to a Compton-scattered electron. These spectra are the result of a self-consistent computation and are not necessarily identical with the actual energy spectra.

distributions, each of which is rectangular in shape. The object of this portion of the calculation is to unfold these Compton distributions to find the energy spectrum of the γ -radiation. The above can be written in mathematical representation as

$$C_J = \sum_{I=J}^N R_{JI} N_I,$$

or in matrix form as

$$[C] = [R] \times [N].$$

Here C_J represents the number of counts in the J th pulse-height bin, N_I is the number of photons impinging on the scintillator having energies whose values lie in the I th energy bin, and R_{JI} is the operator which transforms photon flux into counts in the J th bin. R_{JI} is simply the product of detection efficiency and the number of counts per channel for each event detected. For a rectangular Compton pulse-height spectrum, this is simply the detection efficiency divided by the channel number corresponding to the Compton edge. When the R_{JI} 's are found, the N_I 's are easily determined. The unfolded spectra are shown in Fig. 9. Each histogram has been normalized, so that the areas are identical. It is emphasized that these spectra result

from self-consistent calculations and are not necessarily identical with the actual energy spectra.

C. Correction Factors

The relative number of photon events recorded by the detector for the early and late spectra shown in Fig. 9 is given by

$$C_T = \sum_I \epsilon_I N_I,$$

where ϵ_I is the detection efficiency for the I th energy bin. The correction factor was obtained by taking the ratio of the totals for the two spectra. The result is 1.142,

comparing the early-time spectrum with the late. In applying this correction, it was assumed that for the time region 0.35–4.0 sec, there is no change in the γ -energy spectrum and therefore no correction. For the time domain 0.01–0.35 sec it was assumed that the detection efficiency changed linearly with time. From the above calculation, the resulting correction coefficient was $-0.053\%/msec$. Thus, the correction applied to the 0.01-sec data was 18% and that applied to the 0.35-sec data was zero.

The error assigned to the correction was assumed to be $\pm 50\%$. This error was folded in with the other errors to obtain the error flags shown in Figs. 5 and 6.

Energy-Distribution Measurement in the Double Decay of ^{137}Ba

A. LJUBIČIĆ, B. HRASTNIK, K. ILAKOVAC, V. KNAPP, AND B. VOJNOVIĆ

Institute "Ruer Bošković," Zagreb, Yugoslavia

(Received 28 January 1969)

The energy spectrum in the K -electron-photon double decay of the 662-keV state of ^{137}Ba has been measured at an angle of 27° . The experimental data for photon energies above 70 keV are in good agreement with the theory of Spruch and Goertzel, in which the process is treated in an approximation as the internal Compton effect. At lower energies a disagreement has been found. The contribution of the K -electron-photon double decay proceeding via nuclear intermediate states has been estimated on the basis of previous results on double γ decay, and has been found to be negligible.

INTRODUCTION

IN addition to single-decay processes (γ -ray emission, electron conversion, and emission of an electron-positron pair), nuclear transitions can also proceed via double-decay processes.¹ These involve a simultaneous emission of a photon-conversion-electron pair, of two photons, or of two conversion electrons (at higher energies three other processes involving emission of electron-positron pairs are possible). In this paper we present a measurement of the double decay of the former type of the 622-keV state in ^{137}Ba . This type of double decay has previously been studied by several groups.²⁻⁴ It can proceed via two mechanisms, which differ in whether the real photon is emitted by an intermediate virtual state of the electron or of the nucleus. Spruch and Goertzel⁵ and Melikian⁶ have de-

veloped a theory of the former mechanism, often called the internal Compton effect. Also, calculations of the latter mechanism have been made.⁷ The measurements of the electron-photon angular correlation are in agreement with the theory of Spruch and Goertzel.^{3,4,8} The present measurements of the photon energy distribution represent an independent check of the theory.

EXPERIMENT

The radioactive source was an approximately 40- $\mu\text{g}/\text{cm}^2$ -thick film of ^{137}Cs of about 30 μCi . It was deposited on a Mylar foil approximately 1 mg/cm^2 thick. The external bremsstrahlung of K conversion electrons would yield triple coincidence events, which would be indistinguishable from the electron-photon double-decay events. Lindquist *et al.*³ have investigated the contribution of this effect and have shown it to be negligible for a source of a similar thickness on an aluminium backing.

The experimental arrangement is shown in Fig. 1. The source was mounted in the center of a 22-cm-diam vacuum chamber. A Si(Li) detector 12 mm diam \times 0.9

¹ H. J. Leisi, in Proceedings of the Conference on the Electron Capture and Higher Order Processes in Nuclear Decay, Debrecen, 1968 (unpublished); E. L. Church and T. R. Gerholm, Phys. Rev. **143**, 879 (1966).

² H. B. Brown and R. Stump, Phys. Rev. **90**, 1061 (1953); P. Kleinheinz, L. Samuelsson, R. Vukanović, and K. Siegbahn, Nucl. Phys. **59**, 673 (1964).

³ T. Lindquist, B. G. Pettersson, and K. Siegbahn, Nucl. Phys. **5**, 47 (1958).

⁴ E. Fuschini, C. Maroni, and P. Veronesi, Nuovo Cimento **26**, 831 (1962); **41**, B252 (1966).

⁵ L. Spruch and G. Goertzel, Phys. Rev. **94**, 1671 (1953).

⁶ E. G. Melikian, Zh. Eksperim. i Teor. Fiz. **31**, 1088 (1956) [English transl.: Soviet Phys.—JETP **4**, 930 (1957)].

⁷ J. Eichler, Z. Physik **160**, 333 (1960).

⁸ B. G. Pettersson, in *Alpha-, Beta-, and Gamma-Ray Spectroscopy*, edited by K. Siegbahn (North-Holland Publishing Co., Amsterdam, 1965), p. 1569.